



HAL
open science

Demonstration of an All-Fiber Broadband Optical Parametric Amplifier at 1 μm

M.W. Lee, T. Sylvestre, M. Delqué, Alexandre Kudlinski, Arnaud Mussot,
J.F. Gleyze, A. Jolly, H. Maillotte

► **To cite this version:**

M.W. Lee, T. Sylvestre, M. Delqué, Alexandre Kudlinski, Arnaud Mussot, et al.. Demonstration of an All-Fiber Broadband Optical Parametric Amplifier at 1 μm . *Journal of Lightwave Technology*, 2010, 28 (15), pp.2173 - 2178. 10.1109/JLT.2010.2053195 . hal-00524508

HAL Id: hal-00524508

<https://hal.science/hal-00524508>

Submitted on 19 Apr 2021

HAL is a multi-disciplinary open access archive for the deposit and dissemination of scientific research documents, whether they are published or not. The documents may come from teaching and research institutions in France or abroad, or from public or private research centers.

L'archive ouverte pluridisciplinaire **HAL**, est destinée au dépôt et à la diffusion de documents scientifiques de niveau recherche, publiés ou non, émanant des établissements d'enseignement et de recherche français ou étrangers, des laboratoires publics ou privés.



Distributed under a Creative Commons Attribution 4.0 International License

Demonstration of an All-Fiber Broadband Optical Parametric Amplifier at 1 μm

Min Won Lee, Thibaut Sylvestre, Michaël Delqué, Alexandre Kudlinski, Arnaud Mussot, J.-F. Gleyze, Alain Jolly, and Hervé Maillotte

Abstract—In this paper, an optical parametric amplifier and wavelength converter in an all-fiber optical configuration is experimentally demonstrated for photonic applications in the 1 μm band. This is achieved by using a microstructured fiber which provides anomalous dispersion at 1 μm and an LiNbO_3 electro-optic intensity modulator specially designed at this operating wavelength for generating pump pulses. A gain of greater than 30 dB together with highly efficient wavelength conversion is obtained at 1053 nm. The gain bandwidth and gain-power efficiency are also investigated. Experimental results agree well with the theory of parametric amplification including Raman scattering.

Index Terms—Fiber optical parametric amplifiers, optical fiber amplifiers.

I. INTRODUCTION

FIBER optical parametric amplifiers (FOPAs) have evinced tremendous interest over the years in view of their potential application to all-optical signal processing technologies [1]–[3]. In addition to providing large gain and wide bandwidth, they offer access to arbitrary wavelength ranges, simultaneous wavelength conversion and low noise figures. Much effort has been spent on FOPAs for telecommunication applications in the 1.5 μm wavelength band and some outstanding progress have been made such as 70 dB net gain and bandwidth of a few hundred nanometers in standard and highly-nonlinear dispersion shifted optical fibers [1]. The use of microstructured optical fibers (MOF) in parametric devices such as amplifiers, generators and oscillators has been the subject of much recent work [4]–[7]. MOFs indeed offer the promise of extending the range of attainable wavelengths and efficiency of parametric devices. FOPA in the 1 μm band is also of great interest because of the need of all-optical broadband signal processing techniques for Ytterbium-doped fiber laser and amplifier systems. Recently, an FOPA has been reported in the 1- μm band by

using a MOF that provides anomalous dispersion in the band [8]. This FOPA was demonstrated in free space as a proof of principle and cannot be implemented in practical fiber-based systems. In this work, optical parametric amplification in the 1- μm band is experimentally achieved, for the first time to our knowledge, in a fully integrated all-fiber and polarization-maintaining (PM) optical system, paving the way for practical applications to all-optical pulse processing in the 1- μm window. The FOPA demonstrated in this work is implemented with a pump pulsed by an electro-optic intensity modulator specially designed to operate at 1 μm with a minimum insertion loss, enhanced extinction ratio and a high optical damage threshold. Efficient parametric gain and wavelength conversion are demonstrated by pumping at 1065 nm near the zero-dispersion wavelength of the MOF and by using a signal at a centre-wavelength of 1053 nm. The choice of the signal wavelength, which is located in the anti-Stokes band of the FOPA, matches the specific needs of the search of Inertial Confinement Fusion (ICF) in large laser systems [9], [10]. Our experimental results show a net parametric gain of greater than 30 dB at 1053 nm with a good quality of optical amplification and higher idler wavelength conversion efficiency due to the additional contribution of the Raman gain. This all-fiber pulsed-pump parametric device provides efficient amplification and conversion for applications such as optical parametric chirped-pulse amplification (OPCPA) [11], [12], pulse optical replication or regeneration, ultrafast optical sampling and next generation optical oscilloscopes [13], [14]. These applications may take a large benefit from FOPA to provide a fairly uniform spectral gain over broad bandwidth.

II. EXPERIMENTAL SETUP

Setting an all-fiber PM OPA in the 1- μm band is a big challenge because of the need for low insertion loss fiber optic components, electro-optical modulators and a suitable optical fiber as a nonlinear medium. At such a wavelength, anomalous dispersion can be provide only by the use of a MOF whose photonic crystal cladding ensures a high single-mode field confinement together with the dispersion characteristics [15], [16]. MOF has been widely used for fiber optical parametric oscillators. In our experimental setup shown schematically in Fig. 1, the pump is provided by a 6 mW tunable DFB laser source at 1060 nm with a tuning range from 1040 nm to 1080 nm. The linearly-polarised CW emission of the laser is converted to pulse emission by an LiNbO_3 electro-optic Mach-Zhender intensity modulator manufactured by Photline Technologies (NIR-MX series). The modulator is specially designed for operation at 1060 nm with low insertion loss (- dB), high extinction ratio and high optical

M. W. Lee, T. Sylvestre, M. Delqué and H. Maillotte are with the Département d'optique P. M. Duffieux, Institut FEMTO-ST, Université de Franche-Comté, CNRS UMR 6174, F-25030 Besançon cedex, France (email: thibaut.sylvestre@univ-fcomte.fr).

A. Kudlinski and A. Mussot are with the Laboratoire de Physique des Lasers Atomes et Molécules, IRCICA, Université de Lille 1, CNRS UMR 8523, 59655 Villeneuve d'Ascq Cedex, France.

J.-F. Gleyze and A. Jolly are with the Commissariat à l'Energie Atomique (CEA), Centre d'Etudes Scientifiques et Techniques Aquitaine, Chemin des sablières, 33144 Le Barp, BP2, France.

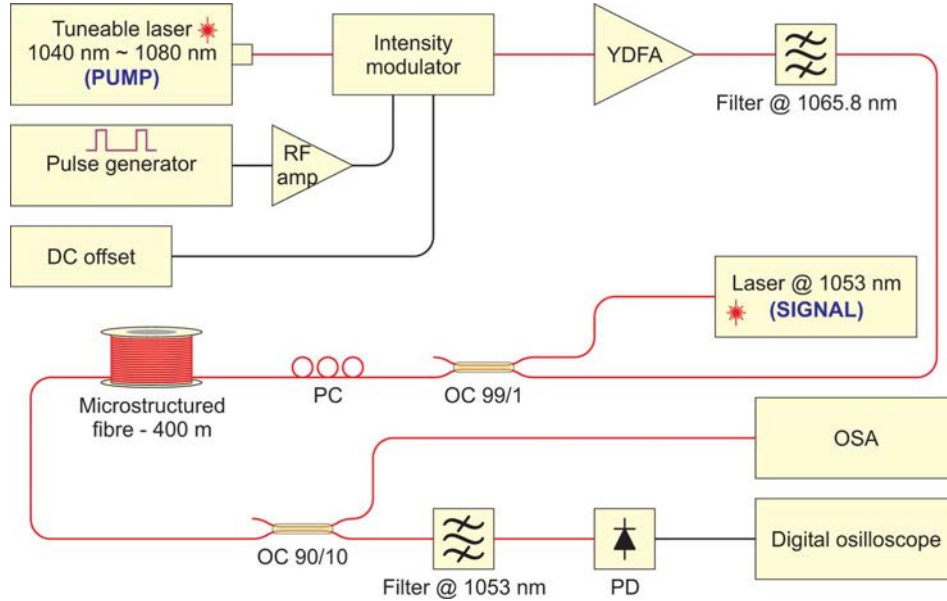


Fig. 1. Schematic diagram of the experimental setup. RF Amp: RF amplifier, YDFA: Ytterbium-doped fiber amplifier, OC: optical coupler, PC: polarisation controller, PD: photodetector, OSA: optical spectrum analyzer. The polarisation is maintained in the whole setup.

damage threshold. A pulse generator is used to generate rectangular pulses and an RF amplifier amplifies pulses so as to drive the modulator over V_{π} of modulation. In this experiment, a short pulse (<10 ns) is used to avoid any Brillouin backscattering that limits the OPA gain [1]. The pulsewidth and duty cycle of pulse train are then set to 3.4 ns and 1/16, respectively. A DC offset is added into the modulator to suppress residual CW emission in the pulse emission. A high-power polarization-maintaining (PM) Ytterbium-doped fiber amplifier (YDFA) amplifies the pump pulse. A bandpass filter with a 2.5 nm of 3 dB-linewidth is adjusted to 1065.8 nm of center-wavelength to ensure suppression of amplified spontaneous emission (ASE) of the YDFA. Another distributed feedback (DFB) PM fiber laser emitting CW at 1053 nm is used as a signal source to be amplified by the fiber OPA. A 99/1 PM fiber optical coupler at 1060 nm is used to couple both the pump and the signal at the MOF's input. Only 1% of the signal power is injected into the fiber amplifier whilst 99% of the pump is injected into the amplifier to keep the pump power at a maximum level. As parametric amplification is polarization dependent, the states of polarization (SOP) of the pump and signal are maintained in the whole system as well as in the MOF by use of PM elements. We additionally use a polarization controller (PC) before the MOF to align both the pump and signal polarisations parallel to one of the birefringent axes of the MOF. The signal power is set to be 40 dB lower than the maximum average pump power. The input signal power is then measured as -15 dBm. The fiber output is split into two outputs by another 90/10 PM fiber optical coupler. The 10% port is sent to an optical spectrum analyzer (OSA) and the 90% port is injected into another bandpass filter centered at the signal wavelength of 1053 nm. The amplified signal is then detected by a photodetector (PD) and recorded by a real-time digital oscilloscope.

The MOF used in this work was specifically designed and manufactured to provide both anomalous dispersion required for phase-matching and a high nonlinear coefficient for efficient

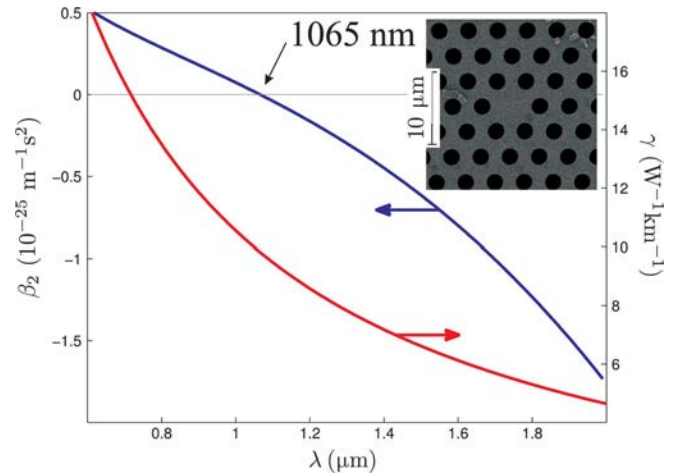


Fig. 2. Dispersion curve for the fundamental mode exhibiting a zero-dispersion wavelength at 1065 nm and nonlinear coefficient as a function of the wavelength. The inner plot shows a SEM image of the microstructured fiber cross-section.

parametric gain. A zoom of the fiber cross section of the MOF is shown in the inset of Fig. 2. The group velocity dispersion coefficient of the fundamental mode has been calculated using a finite element method and is shown in Fig. 2. As seen in the figure, the MOF has a zero-dispersion wavelength (ZDW) close to 1065 nm and a small dispersion slope ($\beta_3 = 0.56$ ps³km⁻¹) at this wavelength. The pitch and hole diameter are 4.14 μ m and 2.61 μ m, respectively. The effective area is measured as $A_{\text{eff}} = 16.2$ μ m² at 1065 nm. Its nonlinearity coefficient is also evaluated as $\gamma = 9.4$ W⁻¹km⁻¹. The optical loss of MOF is measured as 13.5 dB/km at 1060 nm. The 400 m-long MOF used in the setup produces 8.1 dB of optical loss including loss from the fiber splicing at each end with single-mode fiber pigtails. The peak pump power P at the input of MOF is changed by varying the YDFA gain. It is obtained by dividing the average power by

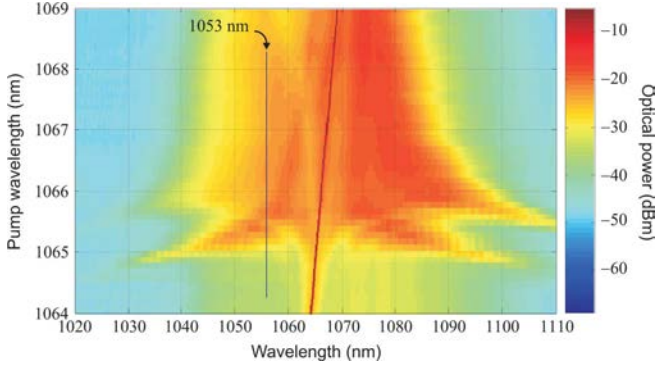


Fig. 3. Color plot of output spectra of the microstructured optical fiber as a function of the pump wavelength and without input signal. The pump power is set to $P = 2.4$ W. The vertical line indicates the signal wavelength used for parametric amplification.

the duty cycle and taking into account the optical loss (-1.25 dB) due to the fiber splicing at the input of FOFA. A peak pump power of as much as 4 W is coupled into the MOF.

III. RESULTS

First, we have performed OPA experiments in the absence of an input signal by tuning the center-wavelength of the pump so as to find the best pump wavelength that provides the maximum parametric gain for the signal at 1053 nm. Fig. 3 depicts the experimental output spectra as a color plot when scanning the pump wavelength from 1064 nm to 1069 nm. Here the power of the YDFA is set to yield approximately 3.6 W of output pump power. The ASE spectra reveal a number of new frequency components created by four-wave mixing (FWM) process at both the sides of the pump wavelength in a range of 1030–1100 nm [16]. We can see in particular a large power asymmetry in the output spectra from 1060 nm pump wavelength. This asymmetry is mainly due to the additional contribution of Raman scattering that leads to higher-power (lower-power) Stokes (anti-Stokes) components [17]–[19]. This combined contribution of both the parametric and Raman gains is significant because the maximum Raman gain is located at 1100 nm. Nevertheless, we are able to identify the maximum ASE power at 1053 nm for a pump wavelength λ_p located at 1065.8 nm. This pump wavelength is kept in the following work.

The peak pump power is now set to $P = 2.4$ W to undertake parametric amplification process in presence of an input signal. Fig. 4 shows input and output spectra of FOFA when pump is switched on and off, respectively. For a fair comparison, the spectra are recorded with the 90/10 optical coupler at the input of OSA. In Fig. 4(a) the pump at $\lambda_p = 1065.8$ nm and signal at $\lambda_s = 1053$ nm are present at the input of FOFA. The signal power at pump-on is measured as -25.4 dBm. The signal power is 40 dB lower than that of the pump. On the other hand, Fig. 4(b) shows -9 dBm of the signal power at the output of FOFA when the pump is on. Comparing these two powers, it is seen that the signal is amplified by 16.4 dB in FOFA. This gain is obtained with the average power of the amplified signal. As the signal is converted from CW to rectangular pulses, the duty cycle of pump pulses needs to be taken into account. The duty cycle is 1/16 and it gives 11.1 dB of extra gain. Hence,

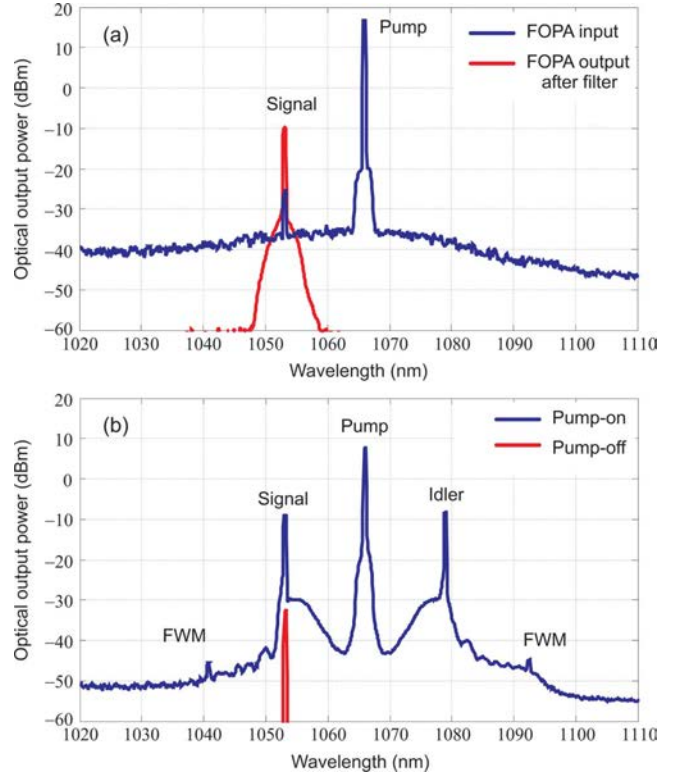


Fig. 4. Spectra of input and output of the microstructured fiber-based OPA for the 1053 nm signal at $P = 2.4$ W. In (a) the blue curve is a spectrum of the FOFA input and the red curve is a spectrum of the FOFA output filtered at 1053 nm. In (b) the blue curve is a spectrum of the FOFA output at pump-on whilst the red curve at pump-off.

this results in 27.5 dB of net gain. The output signal filtered at 1053 nm is also depicted in Fig. 4(a) that shows a good quality of amplification. A gross gain can also be obtained simply by comparing the output signal powers at pump-on and -off from optical spectra in Fig. 4(b). The signal power at pump-off is as low as -33.5 dBm at the output. Therefore, the gross gain of FOFA is obtained as much as 35.6 dB. This difference of 8.1 dB originates from the optical loss in the MOF. In Fig. 4(b), the idler appears at 1079 nm with the similar power to the signal. Cascaded four-wave mixing (FWM) signals also exist at 1040.7 nm and 1092.4 nm, respectively [20]. Second-order cascaded FWM signals can also be observed with the peak power over 3.4 W. Therefore, the FOFA exhibits high wavelength conversion efficiency. Despite of the filter at 1065.8 nm, residual ASE noise from the YDFA still remains at the FOFA input in Fig. 4(a). Due to this input ASE noise, parametric amplified spontaneous emission (ASE) bands are very significant in Fig. 4(b). As the input ASE noise is quite flat, the parametric gain bandwidth of FOFA would be estimated from the parametric ASE noise. This will be discussed later.

Time traces of the amplified signal at the output of FOFA are also measured. The output of FOFA is filtered at 1053 nm to suppress the residual pump and parametric ASE noise and measured by the PD and oscilloscope. Fig. 5 shows time traces of the amplified signal and pulsed pump at $P = 3.6$ W. For the sake of clarity, the time trace of the pump is displaced; the upper trace (blue trace) is the signal trace amplified by the pulsed pump

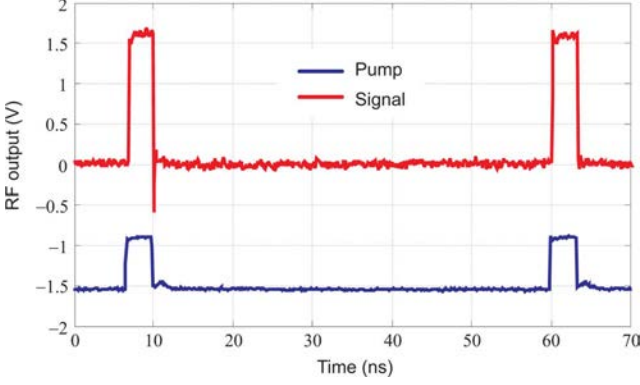


Fig. 5. Time traces recorded by the oscilloscope. The upper trace is a time trace of the signal amplified at $P = 3.6$ W at the output of FOPA. The lower trace is a time trace of the pulsed pump at the input of FOPA. The pump power is attenuated for PD.

at the output of FOPA and the lower trace is the pulsed pump trace at the input of FOPA. The pulsewidth and duty cycle of the amplified signal are measured as 3.4 ns and 1/16, respectively. These values correspond to those of the pump pulses and the signal is transformed to pulses by the pulsed pump. As such, it is clearly shown from the figure that a good quality of parametric amplification is achieved.

The parametric gain efficiency is also investigated with respect to the peak pump power P . Fig. 6(a) displays parametric gains for peak powers P from 0.4 W to 3.8 W. These gains are net parametric gains. The circle dots are parametric gains calculated with optical powers of the signal between input and output spectra of FOPA measured from OSA. On the other hand, the square dots are parametric gains obtained by comparing with RF outputs of the signal from the oscilloscope, i.e., time traces at the output of FOPA. Because of the low sensitivity of the PD, the RF gains below $P = 1.4$ W could not be measured. The negative gains below $P = 1$ W are in fact losses due to 8.1 dB of the fiber loss. The gains after $P = 1.2$ W overcome the fiber loss. As the power increases thereafter, the gains for the 1053 nm signal increases exponentially. However, the gain seems to saturate for the power over 2.8 W. This is because of the pump depletion and particularly parametric ASE noise. In fact, the parametric ASE noise increases significantly above $P = 2.8$ W. It is seen from the figure that the maximum net parametric gain is obtained as 35 dB for the optical gain at $P = 2.8$ W and 32.7 dB for the RF gain at $P = 3.8$ W. By taking into account 8.1 dB of the fiber loss, the maximum gross optical gain can be estimated as 43.1 dB.

Wavelength conversion efficiency of the FOPA is further studied with the idler at 1079 nm. Fig. 6(b) shows optical output powers of the signal and idler measured from optical spectra. The idler power is lower than that of signal below $P = 1.2$ W. However, the idler power overtakes the signal one at $P = 1.2$ W and the idler power is greater than the signal one thereafter. It is speculated that Raman gain involves in the idler power. Although the pump power is estimated below the Raman threshold, a small amount of Raman gain is expected to be present in the idler which is located at 3.2 THz of frequency

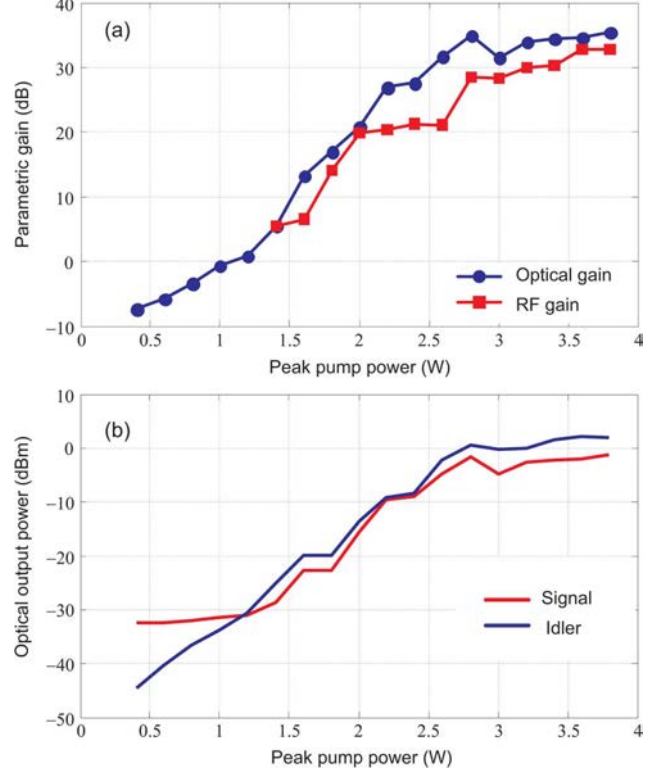


Fig. 6. (a) Net parametric gains with respect to the pump power. Circle dot (blue): parametric gains calculated with powers of the signal from optical spectra. Square dot (red): parametric gains calculated with RF signal outputs from the PD. (b) Optical output power of the signal (blue curve) and the idler (red curve).

offset from the pump. This leads to Raman-assisted parametric frequency conversion, as previously demonstrated [18].

IV. CURVE FITS

In order to compare the experimental measurements with the theory, the gain bandwidth and gain over power are fitted. The theoretical parametric gain is given by [1]

$$G_P(\Omega) = 1 + \left(\frac{\gamma P}{g(\Omega)} \sinh(g(\Omega)L_{\text{eff}}) \right)^2 \quad (1)$$

where $g^2 = (\gamma P)^2 - ((\kappa)/(2))^2$ is the parametric gain factor by unit length, and $\kappa = \beta_2\Omega^2 + \beta_4\Omega^4 + 2\gamma P$, the phase mismatch. $\Omega = 2\pi c(\lambda_s - \lambda_p)/(\lambda_s\lambda_p)$. $\beta_2 = -2\pi c\beta_3(\lambda_p - \lambda_{\text{ZDW}})/\lambda_{\text{ZDW}}^2$ is the group velocity dispersion coefficient at the pump wavelength. β_4 is the fourth-order dispersion as $\beta_4 = -1.06 \cdot 10^{-55} \text{s}^4 \text{m}^{-1}$ obtained from numerical simulations. The fiber length is 400 m, but the effective length is obtained as $L_{\text{eff}} \simeq 229$ m by taking into account the fiber loss [21].

Fig. 6(b) clearly shows output power asymmetry between the signal and idler because of the involvement of Raman gain. The Raman gain is given by [21]

$$G_R(\Omega) = \exp\left(\frac{g_R(\Omega)PL_{\text{eff}}}{A_{\text{eff}}}\right) \quad (2)$$

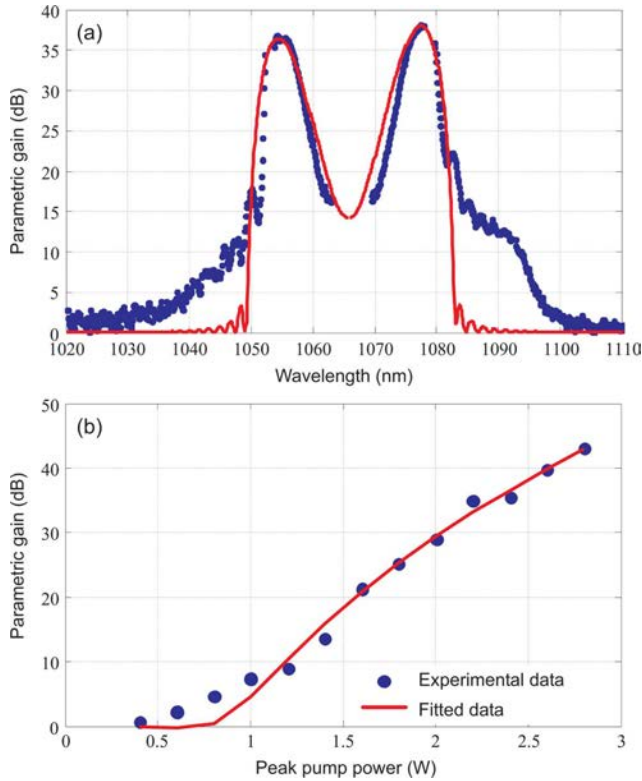


Fig. 7. (a) Gross parametric gain bandwidth. Circle dots (blue): Experimental gain bandwidth extracted from Fig. 4(b). Solid line (red): fitted curve using (3). (b) Gross parametric gain with respect to the peak pump power. Dotted line (blue): parametric gains retrieved from Fig. 6(a). Solid line (red): fitted curve.

where g_R is the Raman gain coefficient for fused silica fiber. As the signal is located on the anti-Stokes side of the pump, we must consider the whole Raman gain including both the anti-Stokes and Stokes gain band [19]. Therefore, the total gain can be approximated by

$$G(\Omega) = G_P(\Omega) + G_R(\Omega). \quad (3)$$

As the laser used for signal generation is not tunable, the experimental gain bandwidth at $P = 2.4$ W can be extracted readily from Fig. 4(b) for the case of gain bandwidth fitting. The extracted gain bandwidth is shown in Fig. 7(a). The signal, pump, idler and FWM sidebands are all suppressed and the gain values are adjusted so that the gain at 1053 nm matches to 35.6 dB of gross gain obtained in Fig. 4(b). Fig. 7(a) also shows in red the fitting curve obtained from (3). In this curve fit, λ_{ZDW} , γ and $g_{R,max}$ are set to be the fitting parameters and obtained as 1065 nm, $9.1 \text{ W}^{-1}\text{km}^{-1}$ and $2 \cdot 10^{-14} \text{ m/W}$ respectively. These values are close to those estimated by a finite element method. By taking into account the whole Raman gain curve including both the anti-Stokes and Stokes bands, the fitted curve in Fig. 7(a) shows a power asymmetry of the gain bandwidth and matches closely to the experimental curve. The idler power is greater than the signal power by around 2 dB. The power asymmetry is similar to the result reported in [19]. From the figure, the gain bandwidth of FOPA is estimated as a range of 1049–1083 nm for the given pump power. This is in good agreement with our previous measurement done in free space [8].

A gain-power curve is obtained from Fig. 6(a) for the case of gain-power fitting. As the gain seems to be saturated beyond $P = 2.8$ W, those values are not considered in the curve fit. The gains in Fig. 7(b) are set to gross gains. The same parameters as in the case of gain bandwidth fitting are used in the fitting. A fitting of gain-power curve gives $\lambda_{ZDW} = 1065.2$ nm, $\gamma = 9.1 \text{ W}^{-1}\text{km}^{-1}$ and $g_R = 2 \cdot 10^{-14} \text{ m/W}$. The ZDW is slightly different to that obtained in the case of gain bandwidth fitting whilst γ remains the same in both the cases.

V. CONCLUSION

In conclusion, we have demonstrated a microstructured fiber-based optical parametric amplifier in a wavelength range near the $1 \mu\text{m}$ band in a fully all-fiber polarization-maintaining optical configuration. This has been achieved using a pump wave pulsed by an LiNbO_3 electro-optic intensity modulator specially designed for operating at 1060 nm. A CW input signal at 1053 nm is converted to a pulsed signal and amplified by the pulsed pump at 1065.8 nm. Maximum net gains of 35 dB and 32.7 dB have been measured both optically and electrically, respectively. From the amplified signal time traces, it is shown that a good quality of parametric amplification has been achieved in terms of optical contrast and temporal stability. By investigating the idler conversion efficiency, it is observed that the idler power is greater than the signal power because of Raman-assisted parametric wavelength conversion. The gain bandwidth of FOPA has also been estimated by means of parametric ASE spectra in a range of 1049–1083 nm. A fitting with the experimental results has given the values of γ and ZDW which are in a good agreement with those estimated from numerical simulations.

The FOPA demonstrated here may be used for optical sampling, optical parametric chirped-pulse amplification (OPCPA) and short pulse processing in the $1\text{-}\mu\text{m}$ Ytterbium band. It is important to stress here that parametric amplification has been undertaken in the continuous-wave pumping regime by use of a phase modulator specially designed at 1060 nm but only 3.5 dB net gain has been obtained. This can easily be improved by reducing the whole optical loss of the fiber optic components and the microstructured fiber, and using the Stokes band instead of the anti-Stokes one of the FOPA. For completeness, we expect in a future work to measure the whole gain bandwidth and the noise figure of the FOPA with a tunable signal source.

ACKNOWLEDGMENT

The authors acknowledge the European INTERREG-IVA programme and the Fond Européen de Développement Régional (FEDER). They thank Photline Technologies for manufacturing the electro-optic modulator.

REFERENCES

- [1] M. E. Marhic, *Fiber Optical Parametric Amplifiers, Oscillators and Related Devices*. Cambridge, U.K.: Cambridge University Press, 2007.
- [2] J. Hansryd, P. A. Andrekson, M. Westlund, J. Lie, and P.-O. Hedekvist, "Fiber-based optical parametric amplifiers and their applications," *IEEE J. Sel. Top. Quantum Electron.*, vol. 8, no. 3, pp. 506–520, May 2002.
- [3] C. J. McKinstrie, S. Radic, and A. H. Gnauk, "All-optical signal processing by fiber-based parametric devices," *Opt. Photon. News*, vol. 18, no. 3, pp. 34–40, 2007.

- [4] J. Fan, A. Dogariu, and L. J. Wang, "Parametric amplification in a microstructure fiber," *Appl. Phys. B*, vol. 81, pp. 801–805, 2005.
- [5] J. E. Sharping, M. Fiorentino, P. Kumar, and R. S. Windeler, "Optical-parametric oscillator based on four-wave mixing in microstructure fiber," *Opt. Lett.*, vol. 27, no. 19, pp. 1675–1677, 2002.
- [6] A. Chen, G. Wong, S. Murdoch, R. Leonhardt, J. Harvey, J. Knight, W. Wadsworth, and P. Russell, "Widely tunable optical parametric generation in a photonic crystal fiber," *Opt. Lett.*, vol. 30, pp. 762–764, 2005.
- [7] J. E. Sharping, "Microstructure fiber based optical parametric oscillators," *J. Lightw. Technol.*, vol. 26, no. 14, pp. 2184–2191, 2008.
- [8] T. Sylvestre, A. Kudlinski, A. Mussot, J.-F. Gleyze, A. Jolly, and H. Maillotte, "Parametric amplification and wavelength conversion in the 1040–1090 nm band by use of a photonic crystal fiber," *Appl. Phys. Lett.*, vol. 94, no. 11, pp. 111104-1–111104-3, 2009.
- [9] D. Besnard, "The megajoule laser program - ignition at hand," *Eur. Phys. J. D*, vol. 44, no. 2, pp. 207–213, 2007.
- [10] C. A. Haynam *et al.*, "National ignition facility laser performance status," *Appl. Opt.*, vol. 46, no. 16, pp. 3276–3303, 2007.
- [11] M. Hanna, F. Druon, and P. Georges, "Fiber optical parametric chirped-pulse amplification in the femtosecond regime," *Opt. Exp.*, vol. 14, no. 7, pp. 2783–2790, 2006.
- [12] C. Caucheteur, D. Bigourd, E. Hugonnot, P. Szriftgiser, A. Kudlinski, M. Gonzalez-Herraez, and A. Mussot, "Experimental demonstration of optical parametric chirped pulse amplification in optical fiber," *Opt. Lett.*, vol. 35, no. 11, pp. 1786–1788, 2010.
- [13] A. Jolly, J.-F. Gleyze, P. Di Bin, and V. Kermène, "Demonstration of a true single-shot 100 GHz-bandwidth optical oscilloscope at 1053–1064 nm," *Opt. Exp.*, vol. 17, no. 14, pp. 12109–12120, 2009.
- [14] P. A. Andrekson, "Ultrahigh bandwidth optical sampling oscilloscope," in *Optical Fiber Communications*, Los Angeles, CA, 2004, no. Paper TuO1.
- [15] P. S. J. Russell, "Photonic crystal fibers," *J. Lightwave Technol.*, vol. 24, no. 12, pp. 4729–4749, 2006.
- [16] W. J. Wadsworth, N. Joly, J. C. Knight, T. A. Birks, F. Biancalana, P. St., and J. Russell, "Supercontinuum and four-wave mixing with *Q*-switched pulses in endlessly single-mode photonic crystal fibres," *Opt. Exp.*, vol. 12, no. 2, pp. 209–309, 2004.
- [17] D. A. Chestnut, C. J. S. de Matos, and J. R. Taylor, "Raman-assisted fiber optical parametric amplifier and wavelength converter in highly nonlinear fiber," *J. Opt. Soc. Amer. B*, vol. 19, no. 8, pp. 1901–1904, 2002.
- [18] T. Sylvestre, H. Maillotte, E. Lantz, and P. Tchofo Dinda, "Raman-assisted parametric frequency conversion in a normally dispersive single-mode fiber," *Opt. Lett.*, vol. 24, pp. 1561–1563, 1999.
- [19] A. S. Y. Hsieh, G. K. L. Wong, S. G. Murdoch, S. Coen, F. Vanholsbeeck, R. Leonhardt, and J. D. Harvey, "Combined effect of raman and parametric gain on single-pump parametric amplifiers," *Opt. Exp.*, vol. 15, pp. 8104–8114, 2007.
- [20] T. T. Ng, J. L. Blows, J. T. Mok, R. W. McKerracher, and B. J. Eggleton, "Cascaded four-wave mixing in fiber optical parametric amplifiers: Application to residual dispersion monitoring," *J. Lightw. Technol.*, vol. 23, no. 2, pp. 818–826, Feb. 2005.
- [21] G. P. Agrawal, *Nonlinear Fiber Optics*. New York: Academic, 2007.